ICECCME 2021
07 - 08 Oct 2021, Mauritius

IEEE
MAURITIUS SECTION

CERTIFICATE OF PARTICIPATION

Presented to

VIKTOR VLASIUK

for an oral presentation in the conference with paper title:

82: KINETICS OF LIGHT-INDUCED PROCESSES DUE TO IRON IMPURITIES IN SILICON SOLAR CELLS

The contribution is awarded with this certificate.

Dr. Emre Arslan
Conference Exacutive Chair

Dr. Mahendra Gooroochurn
Conference Chair

AKSARAY UNIVERSITY 2006

ecer.org
Connect the science

IEEE
MAURITIUS SECTION

IJECER
International Journal of
Electrical and Computer Engineering Research

Kinetics of Light-Induced Processes Due to Iron Impurities in Silicon Solar Cells

Viktor Vlasiuk
Laboratory of Physical and Technical Fundamentals of Semiconductor Photovoltaics
V. Lashkaryov Institute of Semiconductor Physics NAS of Ukraine
Kyiv, Ukraine
viktorvlasiuk@gmail.com

Roman Korkishko
Laboratory of Physical and Technical Fundamentals of Semiconductor Photovoltaics
V. Lashkaryov Institute of Semiconductor Physics NAS of Ukraine
Kyiv, Ukraine
romkin.ua@gmail.com

Vitaliy Kostylyov
Laboratory of Physical and Technical Fundamentals of Semiconductor Photovoltaics
V. Lashkaryov Institute of Semiconductor Physics NAS of Ukraine
Kyiv, Ukraine
vkost@isp.kiev.ua

Oleg Olikh
Faculty of Physics
Taras Shevchenko National University of Kyiv
Kyiv, Ukraine
olikh@univ.kiev.ua

Abstract — **The existing techniques of studying the iron properties in silicon wafers are extended to the case of finished silicon solar cell (SC) at the arbitrary injection level of excess electron-hole pairs in SC. The kinetics of the light-induced processes, in particular the kinetics of open-circuit voltage and short-circuit current, as well as the kinetics of effective lifetime and of the interstitial iron concentration due to the iron-boron pairs dissociation-association reactions are investigated.**

These studies allow us to determine the total iron concentration in our SCs, and to calculate the time constants of the iron-boron pairs photodissociation and association reactions. The obtained time constants are "fingerprints" of iron in silicon. We conclude that the experimentally observed effects in silicon SCs are activated by iron impurities.

Keywords — silicon, solar cells, iron, iron-boron pairs, pair dissociation, recombination

I. INTRODUCTION

The characteristic feature of modern civilization is the persistent increase in energy consumption. Up to now, the growing electricity needs are mainly satisfied by means of fossil energy sources, such as coal, natural gas, oil, nuclear fuel. However, the XXI century is characterized by increasing the share of renewable energy sources, among which photovoltaics, i.e. the direct conversion of solar energy into electricity, holds a special place.

Today there is a great variety of solar cell designs and photovoltaic technologies for their production [1, 2]. The highest confirmed efficiencies and parameters for various types of solar cells are regularly updated in lists [3]. An environ-economic analysis of the three most common PV technologies was presented in [4]. In some countries, namely Italy, Germany, Chile, Japan and others the electricity share generated by the photovoltaic installations exceeds 9% [5, 6], while globally it is 2.7% [6]. The vast majority (>90%) of this energy is provided by silicon solar cells (SC) [6].

The main challenge is to improve the photoconversion efficiency of SCs. To achieve the latter, all types of losses in SCs need to be minimized. One of the most significant losses for both laboratory and mass-produced SCs is the loss due to the recombination of nonequilibrium electron-hole pairs. The level of recombination loss is defined by the type and concentration of impurity atoms. For example, it is known that the heavy metal impurities in silicon act as recombination centers, thus reducing the lifetime of excess current carriers and photoconversion efficiency [7]. One of the most common and harmful impurities in silicon is iron (Fe).

Numerous works have been devoted to understand the properties and influence of iron impurity on the recombination characteristics of silicon. As a result, various methods for determining the Fe concentration have been proposed [8-13]. But most of these researches are focused on the iron impurities in silicon wafers only.

Meanwhile, the effect of the Fe-associated centers on the silicon SC parameters has been typically investigated also on the wafers, prior to SC fabrication. This circumstance appears due to the limitations of the used techniques, such as surface photovoltage (SPV) [8, 9] and quasi-steady-state photoconductivity (QSSPC) [11-13], which are suitable to study the Fe concentration (via the lifetime or diffusion length changes coming from the FeB pairs dissociation-association reactions) in the silicon wafers, but not in SC.

However, the iron properties in the fabricated SC are expected to be essentially different, considering the multilayer and multi-barrier structure of SCs, in contrast to the wafers. This SC structure creates the potential barriers at the boundaries of different (by doping type and level) regions, thus affecting the iron diffusion process. Moreover, during the SC fabrication process, the high-temperature operations are performed, which can either additionally contaminate the device with impurities (including iron), originating from the technological equipment, chemical reagents, etc., or promote the effect of impurities gettering [13]. Therefore, the in-depth researches of the Fe-impurity properties and Fe-activated processes in finished SCs are required.

It is known that Fe in silicon lattice can exist in two forms [8-10, 14-17]:

- as a component of FeB pair (energy level $E_C - 0.27$ eV [17]);

- as an interstitial atom Fe_i (energy level $E_C - 0.735$ eV [17]) that is formed during the FeB pair dissociation.

At room temperature and boron concentration $N_B > 10^{14}$cm^{-3}, all Fe atoms are bounded into FeB pairs and remain in equilibrium, whereas at temperatures above 200°C and $N_B < 10^{16}$cm^{-3}, majority of Fe atoms are in the interstitial state.

It is worth mentioning that Fe_i with its relatively deep energy level is more efficient recombination center than FeB pair with the energy level close to the edge of the valence band. Note that splitting of FeB pairs can be induced by external factors: temperature, irradiation with a photon energy greater than the silicon band gap, etc.

Understanding the physics of the defects and developing the methods to convert these defects into a recombination-inactive state are of fundamental importance to improve SCs performance.

Therefore, in this work we develop a research technique able to determine the concentration of iron impurity in finished silicon SCs, and the impurity effect on the SCs characteristics. Moreover, we explore the kinetics of the light-induced FeB pairs dissociation into an interstitial Fe_i and B atoms, along with the kinetics of the reverse reaction, i.e. Fe_i and B association into pairs.

II. SAMPLES

In these studies, (1.520 x 1.535) cm^2 *p*-type single-crystalline silicon solar cells with base resistivity of 10 Ohm·cm (KDB-10, doping level ~$1.4 \cdot 10^{15}$ cm^{-3}) were used. Initially, thin n^+ (phosphorus) diffused region was formed at the front surface of the 380-μm-thick *p*-type silicon wafer, creating the separating n^+-*p* junction. The isotype p^+-*p* barrier was formed by boron diffusion at the wafer's rear surface, in order to reduce the recombination losses and increase the conductivity of contact layer. Further, the electrical contacts were fabricated in the form of a solid layer of aluminum placed on the rear surface and a grid layer - on the front surface. Additionally, 30-nm-thick SiO_2 and 40-nm-thick Si_3N_4 layers were deposited on the illuminated side of the SC, enabling the surface passivation and optical reflectance reduction.

It should be noted that silicon SCs with a *p*-type base were intentionally selected for the research, because in these SC the lifetime (τ) of the excess current carriers is highly sensitive to the iron impurities concentration (N_{Fe}): τ significantly decreases as N_{Fe} increases. In contrast, in the case of *n*-type base silicon SCs, the presence of iron, even at high concentrations, does not affect the recombination level [18].

III. METHODS

A technique for determining the iron concentration in silicon was first proposed in [8], where, using deep level transient spectroscopy (DLTS), it has been shown that 3-min-long heat treatment of silicon in the dark at 210 °C, results in FeB pairs dissociation and, thus, the interstitial Fe_i emergence.

As a result, the parameters of the iron recombination centers were changed. To track these changes, the measurements of the excess-carriers diffusion length by spectral dependences of surface photovoltage (calibrated using DLTS spectra) have been performed. The following expression for iron concentration in silicon was obtained [8]:

$$N_{Fe} = \frac{D_n}{f}\left(\frac{1}{L_1^2} - \frac{1}{L_0^2}\right) \cdot \left[C_n\left(Fe_i\right) - \frac{C_n(FeB)}{\exp\left(\frac{E_F - 0.1}{kT}\right)}\right]^{-1}, \quad (1)$$

where D_n is the electron diffusion coefficient at room temperature, L_0, L_1 are the diffusion lengths of minority current carriers before and after heat treatment, respectively, C_n (Fe_i), C_n (FeB) are the electron capture coefficients of Fe_i, FeB, respectively, f is the coefficient that takes into account incomplete FeB pairs dissociation, k is the Boltzmann constant, T is the temperature.

Up to now, expression (1) is widely used to determine N_{Fe} in silicon on both laboratory and industrial scales. In particular, it is implemented in the Semilab SDI PV-2000 commercial equipment in the following form:

$$N_{Fe} = 1.05 \cdot 10^{16}\left(\frac{1}{L_1^2} - \frac{1}{L_0^2}\right), \quad (2)$$

where the coefficient $1.05 \cdot 10^{16}$ has the dimension μm^{2}cm^{-3}, and the diffusion length of minority current carriers is expressed in μm.

Subsequently, different approaches to induce the FeB pairs dissociation were suggested. For example, the authors of [14] proposed to expose the sample with the above-silicon-bandgap (1.124 eV) illumination, while in [15, 16] the combination of light and heat treatment was introduced. The latter combined treatment allows to discriminate the contributions to the minority current carriers lifetime changes coming from the iron centers transformation and from the activation-deactivation reactions of boron-oxygen complexes. Table 1 summarizes the effect of various treatment procedures on the light-induced processes in silicon, in accordance with [16].

In order to develop a new technique for studying the kinetics of the iron-impurities-activated light-induced processes in silicon SCs, we performed theoretical calculations of the minority-current-carriers lifetime dependencies upon the excitation level, according to the Shockley-Reed-Hall (SRH) model. For solar cells with a *p*-type base:

$$\tau_{SRH}^p = \frac{\tau_{p0} \cdot (n_1 + \Delta n) + \tau_{n0} \cdot (N_A + p_1 + \Delta n)}{N_A + \Delta n}, \quad (3)$$

where N_A is the doping level, Δn is the concentration of excess nonequilibrium electron-hole pairs (excitation level), $\tau_{p0} = (N_t \sigma_p v_{th})^{-1}$, $\tau_{n0} = (N_t \sigma_n v_{th})^{-1}$, N_t is the concentration of recombination centers, σ_n, σ_p are the cross sections of the recombination center for electrons and holes, respectively, v_{th}^n, v_{th}^p are the average thermal velocities of electrons and holes, which were calculated according to [19],

$n_1 = N_C \cdot \exp\left(-(E_C - E_t)/kT\right)$, $p_1 = N_V \cdot \exp\left(-(E_t - E_V)/kT\right)$, N_C, N_V are the effective densities of states near the bottom of the conduction band and the top of the valence band, respectively [19], E_C, E_V are the energy levels of the bottom of the conduction band and the top of the valence band, E_t is the energy level of the recombination defect.

<div align="center">
TABLE I.   INFLUENCE OF DIFFERENT LIGHT-HEAT TREATMENT COMBINATIONS ON PHOTOINDUCED PROCESSES IN SILICON
</div>

Processing modes			Effect
Temperature	*Light*	*Time*	
Heat treatment			
$\geq 200°C$	no	≥ 2 min.	$Fe_iB \rightarrow \mathbf{Fe_i} + B$
			$\mathbf{BO_{2i}} \rightarrow B + O_{2i}$
FeB Recovery			
90°C	no	≥ 3 min.	$\mathbf{Fe_i} + B \rightarrow Fe_iB$
			B state does not change
Light Induced Degradation Activation			
120°C	1 Sun	≥ 5 min.	$Fe_iB \rightarrow \mathbf{Fe_i} + B$
			$B + O_{2i} \rightarrow \mathbf{BO_{2i}}$

The results of the calculations are shown in Fig. 1. Here, the doping level and the recombination centers' concentration were varied due to iron effect.
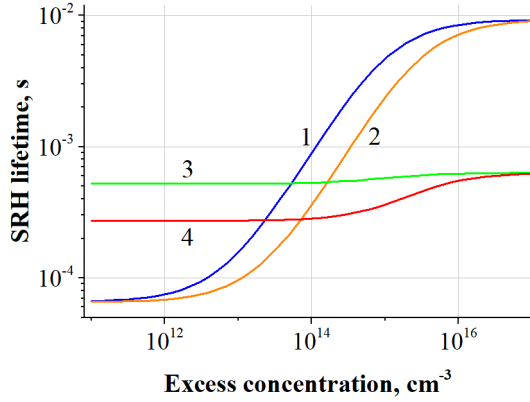

Fig. 1. Dependences of the SRH lifetime in SC base upon the excitation level: curves 1, 2 are for the case of the Fe_i recombination center, $E_C - E_t = 0.735$ eV, $\sigma_n = 3.47 \cdot 10^{-11} \cdot T^{-1.48}$, $\sigma_p = 4.54 \cdot 10^{-16} \exp(-0.05/kT)$ [17], curves 3, 4 are for the case of the FeB recombination center, $E_C - E_t = 0.27$ eV, $\sigma_n = 5.1 \cdot 10^{-9} \cdot T^{-2.5}$, $\sigma_p = 3 \cdot \exp(-0.262/kT)$ [17]. $N_t = 3 \cdot 10^{11}$ см$^{-3}$, $N_A = 10^{15}$ см$^{-3}$ (1, 3) and $3 \cdot 10^{15}$ см$^{-3}$ (2, 4), $T = 298$ K.

As shown in Fig. 1, when the excitation level Δn increases, the SRH lifetime, associated with the recombination level of Fe_i (curves 1 and 2), rapidly increases in the doping range of $2 \cdot 10^{12} - 3 \cdot 10^{15}$ cm^{-3} and remains constant in the doping range of $10^{16} < \Delta n < 10^{12}$ cm^{-3}. On the other hand, the SRH lifetime, associated with the FeB recombination levels (curves 3 and 4), remains constant or increases slightly. Note, the observed rise of the FeB associated SRH lifetime becomes more rapid for the case of SC with the higher doped base (curve 4 in Fig.1).

Thus, Fig. 1 reveals two basic possibilities to investigate the dependencies of the kinetic processes upon iron impurities. The first one is when the excitation levels $< 10^{12}$ cm^{-3}, and the second one - when the excitation levels $> 10^{16}$ cm^{-3}. Note that in both cases, the SRH lifetime changes slightly, providing the high accuracy of the experiment. However, it is difficult to achieve high excitation levels $> 10^{16}$ cm^{-3}, especially for the samples with short lifetimes. Moreover, such excitation levels contribute to undesired sample heating, which strongly affects its characteristics. In addition, as can be seen from Table 1, light treatment with an intensity of 1 Sun already leads to redistribution between FeB and Fe_i. It means that employment of the high irradiation levels aiming to achieve high excitation is able to induce FeB pairs dissociation during the experiment, thus, complicating the analysis of kinetic dependences. Therefore, we suggest to explore the kinetics of the light-induced processes associated with iron impurities in silicon SC at the excitation level that does not exceed 10^{12} cm^{-3}. We also recommend to conduct the studies on SC with a doping level of $10^{15} - 3 \cdot 10^{15}$ cm^{-3}, as in this case the SRH lifetime dependences upon the FeB recombination level are quite insignificant in the whole range of excitation levels.

IV. EXPERIMENT

To study the kinetics of light-induced processes associated with iron impurities in silicon SCs, the light $I–V$ characteristics were measured under the low excitation levels (less than $\Delta n = 10^{11}$ см$^{-3}$) by illuminating the samples with LED. Infrared 950 nm LED (irradiation level of 0.4 mW/cm^2) was chosen to ensure the uniform nonequilibrium electron-hole pairs generation throughout the thickness of SC. By varying the LED current, the $I–V$ characteristics for several excitation levels were obtained.

To track the kinetics of the light-induced FeB pairs dissociation, the $I–V$ characteristics were measured for several stages, including the initial stage, prior to any sample treatment, and further stages, after the performing sequential illumination of the sample with a halogen lamp (1 Sun = 100 mW/cm^2), promoting the FeB pairs dissociation. The latter rearrangement of the defective structure decreases the effective lifetime of nonequilibrium current carriers (Fig. 1), which can be observed from the $I–V$ characteristics.

The time constant τ_p of the FeB pairs association reaction is determined by the following expression [8, 10]:

$$\tau_p = \frac{4.3 \cdot 10^5 T}{N_A} \exp\left(\frac{E_A}{kT}\right) \quad (4)$$

where N_A is the level of boron doping, $E_A = 0.68$ eV is the activation energy of the association reaction $Fe_i + B \rightarrow FeB$. At room temperature, τ_p is too large (> 8 h), so the investigations of the Fe_i and B association kinetics were performed at elevated temperature of $T = 90$ °C, when τ_p decreases to 315 s, according to (4). After the sample temperature was stabilized at 90°C, a 10-min-long halogen lamp (100 mW/cm^2) illumination was implemented in order to dissociate FeB pairs. After the light was switched off, the FeB pairs association kinetics were measured via the light $I–V$ characteristics, similar to that described above. It should be noted that the correspondence of the time constant of the association kinetics to expression (4) at $E_A = 0.68$ eV [8], as

well as pairs photodissociation at room temperatures [9] are "fingerprints" of iron impurities.

As a result, the open-circuit voltage and short-circuit current dependences upon the duration of the halogen lamp illumination (i.e. the kinetics of open-circuit voltage and short-circuit current) are obtained during the dissociation ($FeB \rightarrow Fe_i + B$) and association ($Fe_i + B \rightarrow FeB$) reactions. Next, the nonequilibrium electron-hole pairs effective lifetime kinetics was obtained from the following equation of the generation-recombination balance under the open circuit conditions:

$$J_{SC} = q \frac{d}{\tau_{eff}} \Delta n_{OC},$$ (5)

where J_{sc} is the short-circuit current density, q is the elementary charge, d is the thickness of the SC, τ_{eff} is the effective lifetime of nonequilibrium electron-hole pairs, Δn_{OC} is the excess electron-hole concentration under the open circuit conditions given by the following equation:

$$\Delta n_{OC} = -\frac{n_0}{2} + \sqrt{\frac{n_0^2}{4} + n_i^2 \cdot \exp\left(\frac{V_{OC}}{kT}\right)},$$ (6)

where n_0 is the equilibrium concentration of electron-hole pairs (depends on the doping level of SC), V_{oc} is the open circuit voltage, n_i is the intrinsic concentration of electron-hole pairs in silicon. Note that n_i strongly depends on temperature as the following [20]:

$$n_i(T) = 2.9135 \cdot 10^{15} \cdot T^{1.6} \cdot \exp\left(-\frac{E_g(T)}{kT}\right),$$ (7)

here $E_g(T) = 1.206 - 2.73 \cdot 10^{-4} \cdot T$ is the temperature dependence of the silicon band gap [19].

From (5) we have:

$$\tau_{eff} = \frac{qd\Delta n_{OC}}{J_{SC}}$$ (8)

In addition, using expression (2), the kinetics of the Fe_i concentration (due to the FeB pairs dissociation under the halogen lamp illumination) and the FeB concentration (due to the reverse reaction of association) were obtained. The diffusion length of the minority current carriers L_d was determined as the following:

$$L_d = \sqrt{D\tau},$$ (9)

where $D = 32$ cm^2/s is a diffusion coefficient of minority carriers (electrons).

V. RESULTS AND DISCUSSIONS

The kinetics of open-circuit voltage (V_{oc}) and short-circuit current (I_{sc}) at different excitation levels were obtained through the light $I–V$ measurements conducted at SC prior and after the illumination (halogen lamp with the illumination energy 100 mW/cm^2) treatment. The values of both V_{oc} and I_{sc} exponentially decrease with increasing the illumination duration. Moreover, the maximum drop of the open-circuit voltage due to the light treatment increases with lowering the excitation level, while the maximum drop of the short-circuit current does not depend on the excitation level. Note that

when the light treatment time exceeds 1000 s, both V_{oc} and I_{sc} become saturated and the extended treatment does not have any further effect on them.

Fig. 2 shows the kinetics of the effective lifetime of excess current carriers calculated by using the $I–V$ characteristics (V_{oc} and I_{sc} values) and expressions (5–8). The obtained τ_{eff} kinetics follows the exponential reduction function similar to the V_{oc} and I_{sc} kinetics. Depending on the excitation level, we determine the maximum τ_{eff} values to be in the range from $2.5 \cdot 10^{-7}$ to $2.0 \cdot 10^{-6}$ s, while the minimum τ_{eff} values - from $1.37 \cdot 10^{-8}$ to $1.9 \cdot 10^{-7}$ s. Thus, the maximum τ_{eff} reduction due to the light treatment is about 100% and it decreases slightly with increasing the excitation level.
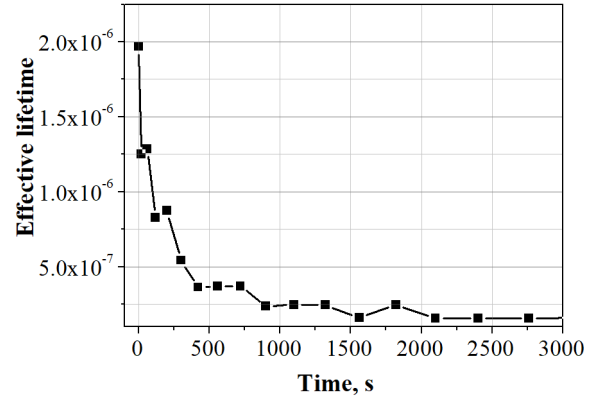

Fig. 2. Kinetics of the effective lifetime of non-equilibrium current carriers in SC under a halogen lamp illumination (100 mW/cm^2). Excess pairs concentration (injection level) $\Delta n = 3 \cdot 10^{10}$ cm^{-3}.

Fig. 3 shows the Fe_i concentration kinetics calculated from expression (2). For this, the minority current carriers diffusion length was obtained at the initial (L_0) and further (L_n) stages of the experiment by substituting the τ_{eff} values from Fig. 2 into the expression (9).
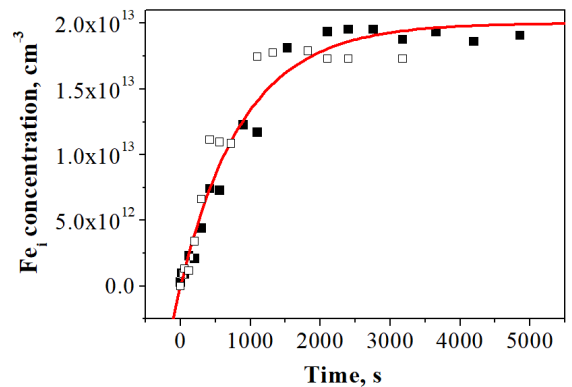

Fig. 3. Kinetics of the interstitial iron Fe_i concentration due to the illumination (halogen lamp, 100 mW/cm^2) induced FeB pairs dissociation. Points are experimental data, solid line is exponential function approximation. Excess carriers concentration (injection level) $\Delta n = 2 \cdot 10^{10}$ cm^{-3} (open squares) and $3 \cdot 10^{10}$ cm^{-3} (closed squares).

In Fig. 3 the solid line represents the exponential approximation (with a time constant of 900 s) of the

experimental data (squares), which are in a good agreement, especially for the first half of the kinetic curve. The complete dissociation of the FeB pairs occurs in about 3000 s (50 min). This value correlates well with the one claimed in [9], where 15 s were obtained at the 100 times higher illumination level (10 W/cm²) of p-Si wafers.

Note that a linear extrapolation of this value of time (15 s) down to 100 mW/cm² illumination level would give 1500 s, which is halved compared to what we obtained for the case of complete FeB pairs dissociation (3000 s). It can be caused by the superlinear effect of the illumination level on the photodissociation, as well as the SC's potential barriers effect. The stationary concentration of interstitial iron $N_{Fei} = 2 \cdot 10^{13}$ cm^{-3} corresponds to the total concentration of iron after the complete FeB pairs dissociation. According to [9], the photodissociation at room temperature is inherent feature of FeB pairs only, in contrast to other metals, in particular CrB.

To further verify that the obtained kinetic dependences are exclusively caused by iron impurities effect, we investigated the kinetics of the reverse reaction that is the association of $Fe_i + B \rightarrow FeB$ pairs [8]. The association kinetics followed after the photodissociation was observed at a temperature of 90 °C [9, 15, 16].

Fig. 4 shows the Fe_i concentration (squares) kinetics due to the FeB pairs association that is well fitted by the exponential function with the association time constant $\tau_p = 315$ s. Note that expression (4) gives the same τ_p value of 315 s at $T = 90°C$. Thus, the kinetics of the FeB pairs association reaction in our SC occurs with an activation energy $E_a = 0.68$ eV, which is a "fingerprint" of iron in silicon. Based on the obtained results, we claim that the processes in silicon SCs, observed during the experiments on kinetics of the FeB pairs association-dissociation, were caused exclusively by iron impurity.

Additionally, we investigated the combined effect of light + heat treatment (Table 2) on the processes of iron association-dissociation in silicon SCs.
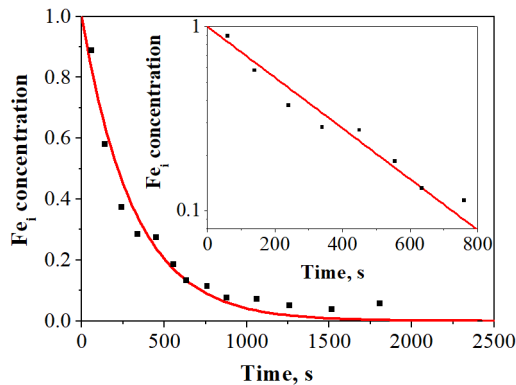

Fig. 4. Kinetics of the interstitial iron Fe_i concentration due to its association with B into FeB pairs. Points are experimental data, solid line is the exponential function approximation with a time constant of 315 s. Inset: a graph on a semi-log scale.

TABLE II.   DIFFUSION LENGTH OF MINORITY CURRENT CARRIERS AT DIFFERENT EXPERIMENTAL STAGES

Stage	Effect	L_d, μm
1. Initial sample		62
2. Thermal treatment 200°C for 2 min.	$Fe_iB \rightarrow \mathbf{Fe_i} + B$ $\mathbf{BO_{2i}} \rightarrow B + O_{2i}$	37
3. Thermal treatment 90°C for 4x3 min.	$\mathbf{Fe_i} + B \rightarrow Fe_iB$ B state does not change	49
4. 120°C and simultaneous illumination with a halogen lamp (100 mW/cm²) for 5 min.	$Fe_iB \rightarrow \mathbf{Fe_i} + B$ $B + O_{2i} \rightarrow \mathbf{BO_{2i}}$	36

Bold letters indicate lifetime decreasing states.

At each stage of the study, the spectral dependences of the short-circuit current $I_{sc}(\lambda)$ were measured in the wavelength range $\Delta\lambda = 800–1200$ nm and at a constant irradiation level. Then, the external and internal quantum efficiencies were obtained from the $I_{sc}(\lambda)$ spectra. The diffusion lengths of minority current carriers (L_d) were determined from the internal quantum efficiency spectra by a method similar to that described in [21]. The obtained L_d values are shown in Table 2. Here, the difference in L_d between stages 2 and 3 is due to Fe_i and B association into FeB pairs, while the similar L_d values obtained at stages 2 and 4, indicate an insignificant effect of BO_{2i} complexes. However, it should be noted that heat treatment at 90°C for 3 min (stage 3) does not lead to the complete recovery of the SC characteristics to the initial values; most likely it is due to the incomplete recovery of FeB bonds, destroyed at stage 2 (heat treatment at 200°C for 2 min), after stage 3 (heat treatment at 90°C for 3 min). Our further studies show that a series of successive heat treatments at 90°C for 3 min each lead to a gradual return of the SC characteristics to their original values.

VI. CONCLUSIONS

We propose the approach able to extend the existing techniques of studying the iron properties in silicon wafers to the case of finished silicon solar cell (SC) at the arbitrary injection levels of excess electron-hole pairs. Using this approach, the kinetics of light-induced processes, in particular the kinetics of open-circuit voltage and short-circuit current, as well as the kinetics of effective lifetime and of the interstitial iron Fe_i concentration due to the FeB pairs dissociation-association reactions have been investigated. Moreover, the total concentration of iron in the studied SCs, as well as the time constants of the photodissociation (3000 s at 100 mW/cm²) and association (315 s at T = 90 °C) kinetics of pairs were determined. These time constants are "fingerprints" of iron in silicon. Thus, we conclude that the experimentally observed processes in silicon SC are exclusively caused by iron impurities. It is also shown that iron impurities lead to the significant reduction of the effective lifetime of excess current carriers, which causes a decrease in the open-circuit voltage and short-circuit current in p-silicon SCs used in this study.

REFERENCES

[1] M. A. Green, "Photovoltaic technology and visions for the future," Prog. Energy, vol. 1, No. 1, 2019, pp. 013001:1-13.

[2] G. M. Wilson et al, "The 2020 photovoltaic technologies roadmap," J. Phys. D: Appl. Phys., vol. 53, 2020, pp. 493001:1-47.

[3] M. Green, E. Dunlop, J. Hohl-Ebinger, M. Yoshita, N. Kopidakis, X. Hao, "Solar cell efficiency tables (version 57)," Prog. Photovolt. Res. Appl., vol. 29, 2021, pp. 3–15.

[4] Pramod Rajput, Maria Malvoni, Nallapaneni Manoj Kumar, O. S. Sastry and Arunkumar Jayakumar "Operational Performance and Degradation Influenced Life Cycle Environmental–Economic Metrics of mc-Si, a-Si and HIT Photovoltaic Arrays in Hot Semi-arid Climates," Sustainability, vol. 12, No. 3, 2020, 1075.

[5] https://ourworldindata.org/grapher/share-electricity-solar

[6] https://www.ise.fraunhofer.de/content/dam/ise/de/documents/publications/studies/Photovoltaics-Report.pdf

[7] A. Rohatgi, Rai-Choudhuri, "High-efficiency silicon solar cells Development, current issues and future directions," Solar Cells 17, pp. 119-133 (1986).

[8] G. Zoth, W. Bergholz, "A fast, preparation-free method to detect iron in silicon," J. Appl. Phys. 67(11), pp. 6764-6771 (1990).

[9] J.Lagowski, P.Edelman, A.M.Kontkiewicz, O. Milic, W. Henley, M. Dexter, L. Jastrzebski, A.M. Hoff, "Iron detection in the part per quadrillion range in silicon using surface photovoltage and photodissociation of iron-boron pairs," Appl. Phys. Lett. **63** (22) 1993 3043-3045

[10] W. Wijaranakula, "The Reaction Kinetics of Iron-Boron Pair Formation and Dissociation in P-Type Silicon," J. Electrochem. Soc., Vol. 140, No. 1, January 1993, p.275-281

[11] D. H. Macdonald, L. J. Geerligs, A. Azzizi, "Iron detection in crystalline silicon by carrier lifetime measurements for arbitrary injection and doping," Journal of Appl.Phys. -2004.-V.95, No3.- P.1021-1028.

[12] J. Tan, D. Macdonald, F. Rougieux and A. Cuevas, "Accurate measurement of the formation rate of iron–boron pairs in silicon," Semicond. Sci. Technol. 26 (5) 055019 (2011)

[13] D. Macdonald, H. Mäckel, and A. Cuevas "Effect of gettered iron on recombination in diffused regions of crystalline silicon wafers," Appl. Phys. Lett. 88, 092105 1-4 (2006)

[14] D. Walz, J.-P. My, G. Kamarinos, "On the recombination behaviour of iron in moderately boron-doped p-type silicon," Appl. Phys. A: Mater. Sci. Process. 62(4), pp. 345-353 (1996).

[15] M. Wilson, P. Edelman, A. Savtchouk, J. D'Amico, A. Findlay, J. Lagowski,"Accelerated light-induced degradation (ALID) for monitoring of defects in PV silicon wafers and solar cells," J. Electron. Mater. 39, pp. 642-647. 31 (2010).

[16] M. Tayyib, J. Theobald, K. Peter, J.O. Odden, T.O. Sætre, "Accelerated light-induced defect transformation study of Elkem solar grade silicon," Energy Procedia 27, pp. 21-26 (2012).

[17] B. B. Paudyal, K. R. McIntosh, D. H. Macdonald, "Temperature dependent electron and hole capture cross sections of iron-contaminated boron-doped silicon," 34th IEEE Photovoltaic Specialists Conference (PVSC), USA, Philadelphia, 7-12 June 2009.

[18] A.V. Sachenko, V.P. Kostylyov, M.V. Gerasymenko, R.M. Korkishko, M.R. Kulish, M.I. Slipchenko, I.O. Sokolovskyi, V.V. Chernenko, "Analysis of the silicon solar cells efficiency. Type of doping and level optimization," Semiconductor Physics, Quantum Electronics & Optoelectronics 19(1), pp. 67-74 (2016).

[19] M. A. Green, "Intrinsic concentration, effective densities of states, and effective mass in silicon," J. Appl. Phys. 67(6), pp. 2944-2954 (1990).

[20] T. Trupke, M. Green, P. Wurfel, P. P. Altermatt, A. Wang, J. Zhao, and R. Corkish, "Temperature dependence of the radiative recombination coefficient of intrinsic crystalline silicon," J. Appl. Phys. 94(8), pp. 4930-4937 (2003).

[21] ASTM Standard F391-90a, "Standard Test Method for Minority-Carrier Diffusion Length in Silicon by Measurement of Steady-State Surface Photovoltage", 1996 Annual Book of ASTM Standards, Am. Soc. Test. Mat., West Conshohocken, PA, 1996.